**Soils and Rocks**
*An International Journal of Geotechnical and Geoenvironmental Engineering*
www.soilsandrocks.com
ISSN 1980-9743
ISSN-e 2675-5475

# Parameters controlling the expansive behavior of bentonite-kaolin mixtures stabilized with alkali-activated waste

Mariana Tonini de Araújo[1], Suéllen Tonatto Ferrazzo[1], Giovani Jordi Bruschi[1#], Nilo Cesar Consoli[1]

**Article**

**Keywords**
Sugarcane bagasse ash
Hydrated eggshell lime
Alkaline cement
Expansive soils
Swelling

## Abstract

Expansive soils can cause large-scale damage to the infrastructure. Soil stabilization with Portland cement and lime has been widely utilized as a solution to this problem. However, these stabilizers are non-renewable and energy-intensive. Alkali-activated binders are alternatives with lower carbon dioxide emissions. This research evaluated an expansive soil stabilization with an alkali-activated binder produced from sugarcane bagasse ash (SCBA), hydrated eggshell lime (HEL) and sodium hydroxide (NaOH). Free-swelling tests alongside a statistical analysis evaluated the influence of dry unit weight (12.5 and 14.5 kN/m$^3$), binder (4 and 10%) and moisture content (19.7 and 24.7%) and curing time (0 and 7 days) on the stabilized mixtures. A four factors factorial design with duplicates and central points was outlined. To better understand the NaOH and SCBA influence over the soil expansion additional tests were performed. In general, an increase on the studied factors reduced swelling, especially binder content. However, the alkali-activated cement presented no clear correlation between higher density and higher expansion. Swell reduced from 13.8% (12.5 kN/m$^3$ and 19.7% moisture) and 8.8% (12.5 kN/m$^3$ and 24.7% moisture) to 2.5% and 0%, respectively, after 7 days and 10% binder addition for the alkaline cement. For Portland cement, swell reduced from 13.8% (10.2 kN/m$^3$ and 22.5% moisture) and 12.5% (10.2 kN/m$^3$ and 27.5% moisture) to 1.8% and 1%, respectively, after 7 days and 4% binder addition. Samples containing NaOH expanded less than samples molded with only water. Finally, the alternative binder might be a viable option to replace Portland cement for expansion control.

## 1. Introduction

Expansive soils suffer considerable volume changes upon the variation of their water content (Consoli et al., 2021; Ferreira et al., 2013; Silvani et al., 2023; Tonini de Araújo et al., 2021). The magnitude of volume change depends on several factors, e.g. mineralogy, type of clay, clay content, and exchangeable ions (Yang et al., 2020), and cause large-scale damage to infrastructure (e.g. roads, buildings, foundations) resulting in economic and safety issues (Gaspar et al., 2022; Yaghoubi et al., 2021). Common solutions to these issues are soil replacement and soil stabilization; due to lower costs associated to the latter, soil stabilization is often preferred in engineering practice (Buhler & Cerato, 2007).

The stabilization of expansive soils with cementing agents such as ordinary Portland cement (OPC) (Abdelkrim & Mohamed, 2013; Ahmadi Chenarboni et al., 2021; Mahedi et al., 2018; Sahoo & Prasad Singh, 2022) and lime (Boobalan & Sivakami Devi, 2022; Dang et al., 2016; Indiramma et al., 2020; James, 2020; James et al., 2022; Khadka et al., 2020) has been widely explored. However, these conventional stabilizers are energy-intensive materials, generate significant amounts of $CO_2$, and possess high costs associated with their production processes (Burris et al., 2015; Gartner & MacPhee, 2011; Zhang et al., 2020). Thus, alternative materials and/or techniques for expansive soils stabilization are needed.

Alkali-activated materials are alternatives to conventional cementing agents. These binders present lower carbon dioxide emissions compared to lime and cement (Zhang et al., 2020) and incorporate several industrial and agro-industrial wastes, such as: sugarcane bagasse ash (Bruschi et al., 2021b, 2022); carbide lime (Carvalho Queiróz et al., 2022; Pereira dos Santos et al., 2022; Queiróz et al., 2022); ground glass waste (Secco et al., 2021), fly ash (Miranda et al., 2020; Goldoni et al., 2023), eggshell residue (Ferrazzo et al., 2023a, b; Levandoski et al., 2023) and, rice husk ash (Pelissaro et al., 2023). Alkali-activation is the chemical reaction between an

---

[#] Corresponding author. E-mail address: gio.bruschi@gmail.com
[1] Universidade Federal do Rio Grande do Sul, Programa de Pós-graduação em Engenharia Civil, Porto Alegre, RS, Brasil.

Submitted on September 19, 2023; Final Acceptance on April 12, 2024; Discussion open until February 28, 2025.
https://doi.org/10.28927/SR.2024.010023

amorphous/semi-crystalline aluminosilicate source and an alkaline activator, generating gel similar to the ones formed in OPC hydration (Duxson et al., 2007).

Past research has been conducted on the use of alkali-activation for the stabilization of problematic soils (Parhi et al., 2018; Phougat, 2015; Samuel et al., 2020; Syed et al., 2020, 2022; Žurinskas et al., 2020). Nevertheless, a research gap exists regarding the application of alkali-activated waste materials to control expansive soils swelling. Thus, this research analyzed the stabilization of an expansive soil by an alkali-activated binder composed by sugarcane bagasse ash and eggshell lime. Free-swelling tests were performed on soil-alkali activated binder samples and a statistical analysis evaluated the influence of studied factors (e.g. curing period) on swelling results.

## 2. Materials and methods

### 2.1 Materials and characterization

The materials used in this research were (i) bentonite, (ii) kaolin, (iii) sugarcane bagasse ash (SCBA), (iv) hydrated eggshell lime (HEL), and (v) sodium hydroxide (NaOH). The sodium bentonite is classified as CH (inorganic clay of high plasticity) and kaolin as CL (inorganic clay of low plasticity) in accordance with USCS (ASTM, 2020). The SCBA was obtained from a local supplier in southern Brazil. HEL was produced from the calcination of eggshells obtained in bakeries. Specifications of the lime production process can be found in Tonini de Araújo et al. (2021). The alkali-activator was NaOH (micro pearls, 98% purity). The materials physical characterization is presented in Table 1.

Bentonite consists of 64.74% $SiO_2$, 13.25% $Al_2O_3$, smectite, and quartz minerals. Kaolin consists of 52.50% $SiO_2$, 31.75% $Al_2O_3$, and kaolinite mineral (Consoli et al., 2021). SCBA consists of 60.65% $SiO_2$, 13.87% $Fe_2O_3$, 5.76% $Al_2O_3$, quartz, hematite, and magnetite minerals (Bruschi et al., 2021a). HEL consists of CaO (72.90%), portlandite, calcite, and magnesium minerals (Consoli et al., 2020).

Previously developed and characterized by Tonini de Araújo et al. (2023a), the alkali-activated binder was composed by 80% SCBA and 20% HEL, 1M NaOH solution (2.61% $Na_2O$), and water/binder rate equal to 0.8.

Modified Proctor tests (ASTM D1557 (ASTM, 2012)) were performed for bentonite-kaolin-SCBA-HEL samples to define the dry unit weight and moisture content of the mixtures (Figure 1). Bentonite-kaolin proportion of 10/90 was established to simulate an expansive soil. The compaction curves resulted in the following maximum dry unit weights and optimum moisture contents: 14.50 kN/m$^3$ and 27.60% (soil), 12.50 kN/m$^3$ and 24.70% (soil-10% binder). The moulding points represent the dry unit weight and respective moisture content applied to the tested samples as described in item 2.2.

### 2.2 Experimental design

A four factors factorial design with duplicates (24) and central points (i.e. 36 tests) was outlined for this study. Analyzed factors were dry unit weight (*A*), binder content (*B*), moisture content (*C*), and curing time (*D*). The experimental runs are shown in Table 2.

To better understand the sodium hydroxide and SCBA influence over the soil expansion additional tests were performed, as described in Table 3. These tests entailed samples with soil and isolated materials.

**Table 1.** Physical properties of the materials.

| Physical properties | Standard/Equipment | Materials | | | |
|---|---|---|---|---|---|
| | | Bentonite (*BT*) | Kaolin (*K*) | SCBA | HEL |
| Unit weight of grains (g.cm$^{-3}$) | ASTM D854 (ASTM, 2014a); NBR 16605 (ABNT, 2017) | 2.75 | 2.61 | 2.08 | 2.24 |
| Liquid limit, *LL* (%) | ASTM D4318 (ASTM, 2017) | 501 | 43 | - | - |
| Plastic limit, *PL* (%) | ASTM D4318 (ASTM, 2017) | 66 | 13 | - | - |
| Plasticity index, *PI* (%) | ASTM D4318 (ASTM, 2017) | 436 | 30 | - | - |
| % of coarse sand | ASTM D7928 (ASTM, 2021) | 0 | 0 | - | - |
| % of medium sand | ASTM D7928 (ASTM, 2021) | 0 | 0 | - | - |
| % of fine sand | ASTM D7928 (ASTM, 2021) | 6 | 4 | - | - |
| % of silt | ASTM D7928 (ASTM, 2021) | 30 | 67 | - | - |
| % of clay | ASTM D7928 (ASTM, 2021) | 64 | 29 | - | - |
| Main particle diameter, $D_{50}$ (µm) | Laser diffraction particle size analyzer (CILAS, model 1064) | - | - | 31.01 | 7.43 |
| Specific surface area (m$^2$.g$^{-1}$) | QuantaChrome equipment (model NOVA 1200e) | - | - | 125.15 | 4.18 |
| Pozzolanic activity index (mg $Ca(OH)_2$/g of pozzolan) | NBR 15895 (ABNT, 2010) | - | - | 817.6 | - |

## 2.3 Molding and curing of soil-binder samples

From Proctor results (Figure 1) the maximum *γd* adopted was 14.5 kN/m$^3$ (maximum γd of the soil-10% binder curve) and the minimum 12.5 kN/m$^3$. For moisture content, the optimum content of 24.7% was the maximum adopted value, and 19.7% the minimum. The binder contents of 10% and 4% were chosen following previous researches (Consoli et al., 2021; Zhang et al., 2013).

The dry unit weight determined the dry mass of materials; after materials weighing, bentonite, kaolin, SCBA, and HEL were mixed, followed by NaOH solution and distilled water addition. The added NaOH solution was defined from an optimum 2.61% alkali content value obtained from SCBA-HEL-NaOH pastes. Additional water aimed to reach the moisture content of the mixture. Next, each sample was statically compacted in a single layer inside a ring (71.33 mm in diameter, 25 mm high). Finished the molding process, each specimen was weighed and specimens suitable for testing met the following tolerances: *γd* within ± 1% of target value, and moisture content within ± 0.5% of target value. Then, samples were stored in a plastic bag to avoid humid loss and cured in a humid chamber (23 ±2°C and 95% moisture).

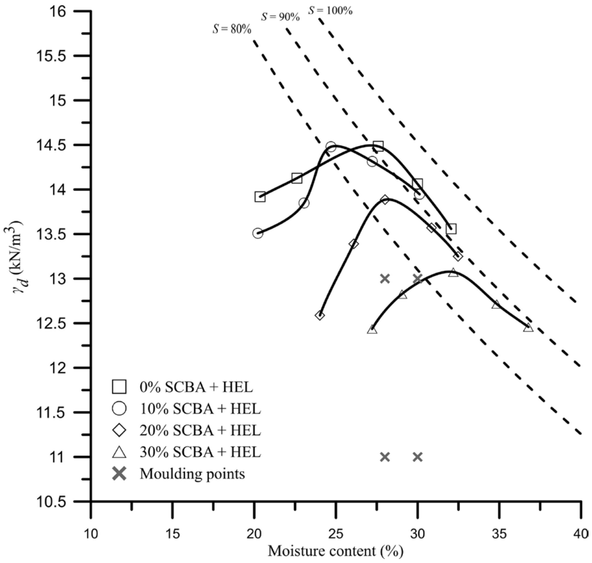

**Figure 1.** Compaction curves.

## 2.4 One-dimensional swell test

The one-dimensional swelling test followed standard ASTM D4546 (ASTM, 2014b), Method A. Each specimen was allocated in a modified odometer cell, with top and bottom saturated porous stones and filter papers, and preloaded by a 1kPa top cap. Next, specimens were inundated using distilled water (20 ± 2°C). A LVDT device coupled to a data acquisition system measured swell at time intervals of 30 s, 1 min, 2 min, 4 min, 8 min, 15 min, 30 min, 1 h, 2 h, 4 h, 8 h, 24 h, and 48 h following the aforementioned standard. The swell percentage is then measured (Equation 1):

$$\varepsilon_s = \frac{\Delta H}{H_0} \times 100 \tag{1}$$

Where $\Delta H$ is the specimen height change (mm) and $H_0$ is the initial specimen height (i.e. the ring height of 25mm).

**Table 2.** Experimental design.

| Treatment | $\gamma_d$ (kN/m$^3$) | Binder content (%) | Moisture content (%) | Curing time (days) |
|---|---|---|---|---|
| 1; 17 | 12.5 | 4% (3.2% SCBA + 0.8% HEL) | 19.7 | 0 |
| 2; 18 | 14.5 | 4% (3.2% SCBA + 0.8% HEL) | 19.7 | 0 |
| 3; 19 | 12.5 | 10% (8% SCBA + 2% HEL) | 19.7 | 0 |
| 4; 20 | 14.5 | 10% (8% SCBA + 2% HEL) | 19.7 | 0 |
| 5; 21 | 12.5 | 4% (3.2% SCBA + 0.8% HEL) | 24.7 | 0 |
| 6; 22 | 14.5 | 4% (3.2% SCBA + 0.8% HEL) | 24.7 | 0 |
| 7; 23 | 12.5 | 10% (8% SCBA + 2% HEL) | 24.7 | 0 |
| 8; 24 | 14.5 | 10% (8% SCBA + 2% HEL) | 24.7 | 0 |
| 9; 25 | 12.5 | 4% (3.2% SCBA + 0.8% HEL) | 19.7 | 0 |
| 10; 26 | 14.5 | 4% (3.2% SCBA + 0.8% HEL) | 19.7 | 7 |
| 11; 27 | 12.5 | 10% (8% SCBA + 2% HEL) | 19.7 | 7 |
| 12; 28 | 14.5 | 10% (8% SCBA + 2% HEL) | 19.7 | 7 |
| 13; 29 | 12.5 | 4% (3.2% SCBA + 0.8% HEL) | 24.7 | 7 |
| 14; 30 | 14.5 | 4% (3.2% SCBA + 0.8% HEL) | 24.7 | 7 |
| 15; 31 | 12.5 | 10% (8% SCBA + 2% HEL) | 24.7 | 7 |
| 16; 32 | 14.5 | 10% (8% SCBA + 2% HEL) | 24.7 | 7 |
| 33; 34; 35; 36 | 13.5 | 7+ (5.6% SCBA + 1.4% HEL) | 22.2 | 3.5 |

**Table 3.** Additional tests.

| Test | $\gamma_d$ (kN/m$^3$) | Binder content (%) | Moisture content (%) | Curing time (days) |
|---|---|---|---|---|
| Soil + $H_2O$ | 12.5 | - | 19.7 | 0 |
| Soil + $H_2O$ | 14.5 | - | 19.7 | 0 |
| Soil + $H_2O$ | 12.5 | - | 24.7 | 0 |
| Soil + $H_2O$ | 14.5 | - | 24.7 | 0 |
| Soil + NaOH | 12.5 | - | 19.7 | 0 |
| Soil + NaOH | 14.5 | - | 19.7 | 0 |
| Soil + NaOH | 12.5 | - | 24.7 | 0 |
| Soil + NaOH | 14.5 | - | 24.7 | 0 |
| SCBA + Soil + $H_2O$ | 12.5 | 4% (3.2% SCBA + 0.8% HEL) | 19.7 | 0 |
| SCBA + Soil + $H_2O$ | 14.5 | 4% (3.2% SCBA + 0.8% HEL) | 19.7 | 0 |
| SCBA + Soil + $H_2O$ | 12.5 | 10% (8% SCBA + 2% HEL) | 19.7 | 0 |
| SCBA + Soil + $H_2O$ | 14.5 | 10% (8% SCBA + 2% HEL) | 19.7 | 0 |
| SCBA +$H_2O$ | - | - | 19.7 | - |
| SCBA +$H_2O$ | - | - | 24.7 | - |

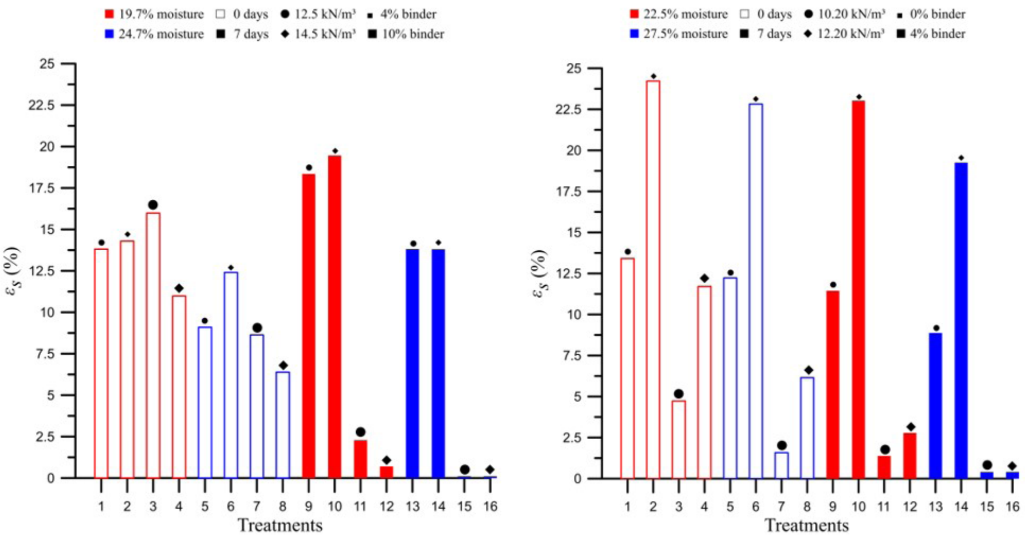

(a) (b)

**Figure 2.** Free swelling: (a) soil-alkali-activated binder, (b) soil-Portland cement (Consoli et al., 2021).

### 2.5 *pH* tests

The *pH* of soil-NaOH and soil-water samples was measured in accordance with ASTM D4972 (ASTM, 2013).

## 3. Results and discussions

Figure 2 shows the free swelling results. Figure 2a presents the mean of the duplicates for each treatment. For comparison with a traditional binder, swelling results for the same soil stabilized by high initial strength Portland cement (type III) (Consoli et al., 2021) are shown in Figure 2b. Although in the later factors values are different from the ones in this study (Table 4), factors influence over swelling results are compared for both binders. Figure 3 presents the Pareto chart and the main effects plot and Figure 4 shows free swelling results over time.

According to Figure 2, a higher moisture content decreased swell. This is due a decrease in suction effects with higher soil saturation, and, consequently, a reduction in soil affinity for water adsorption, as acknowledge by Fattah et al. (2017). In soil-Portland cement samples (0% and 4% cement addition) an increase in density led to higher expansion, as samples that are more compact have lower porosity and less available volume for particles to rearrange after swelling. Also, as stated by Silvani et al. (2020) higher densities result

**Table 4.** Experimental run for the swelling tests of soil-Portland cement samples.

| Treatment | $\gamma_d$ (kN/m³) | Binder content (%) | Moisture content (%) | Curing time (days) |
|---|---|---|---|---|
| 1 | 10.2 | 0 | 22.5 | 0 |
| 2 | 12.2 | 0 | 22.5 | 0 |
| 3 | 10.2 | 4 | 22.5 | 0 |
| 4 | 12.2 | 4 | 22.5 | 0 |
| 5 | 10.2 | 0 | 27.5 | 0 |
| 6 | 12.2 | 0 | 27.5 | 0 |
| 7 | 10.2 | 4 | 27.5 | 0 |
| 8 | 12.2 | 4 | 27.5 | 0 |
| 9 | 10.2 | 0 | 22.5 | 7 |
| 10 | 12.2 | 0 | 22.5 | 7 |
| 11 | 10.2 | 4 | 22.5 | 7 |
| 12 | 12.2 | 4 | 22.5 | 7 |
| 13 | 10.2 | 0 | 27.5 | 7 |
| 14 | 12.2 | 0 | 27.5 | 7 |
| 15 | 10.2 | 4 | 27.5 | 7 |
| 16 | 12.2 | 4 | 27.5 | 7 |
| 17 | 11.2 | 2 | 25.0 | 3.5 |

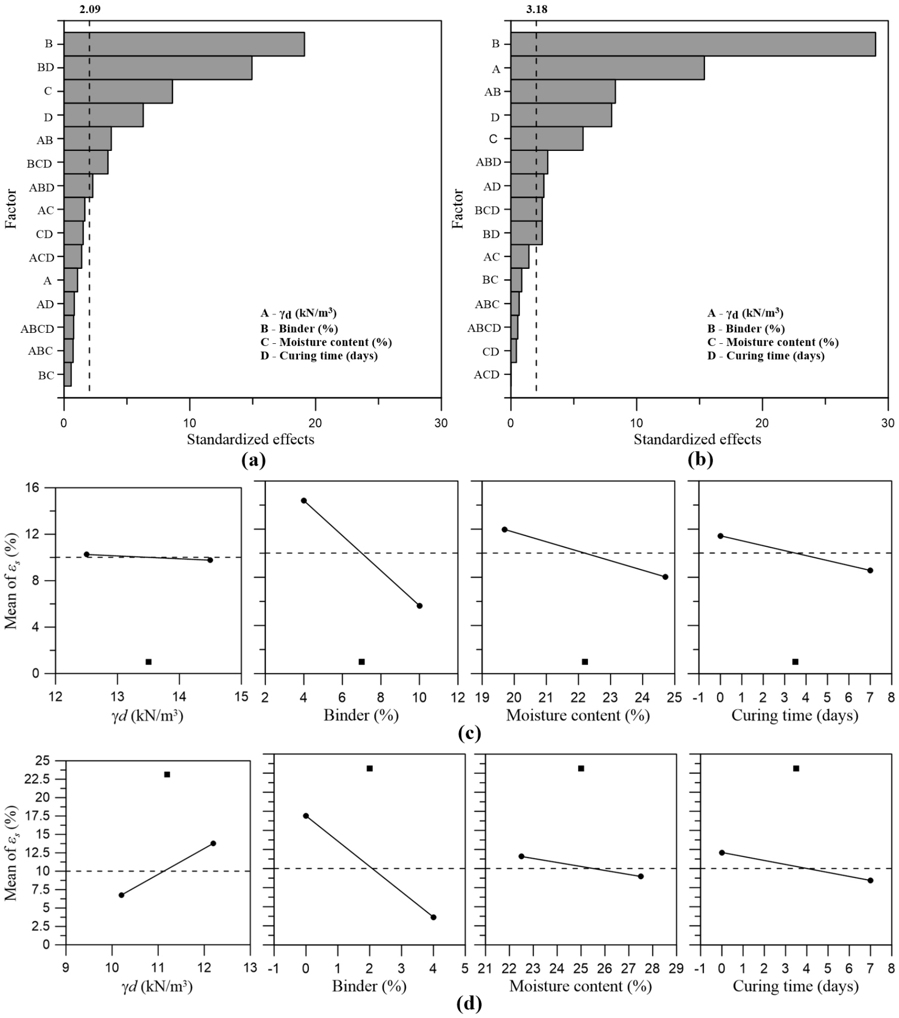

**Figure 3.** Free swelling statistical results: (a) Pareto chart for the soil-alkali-activated binder, (b) Pareto chart for the soil-Portland cement, (c) mean effects plot for the soil-alkali-activated binder, (d) mean effects plot for the soil-Portland cement.

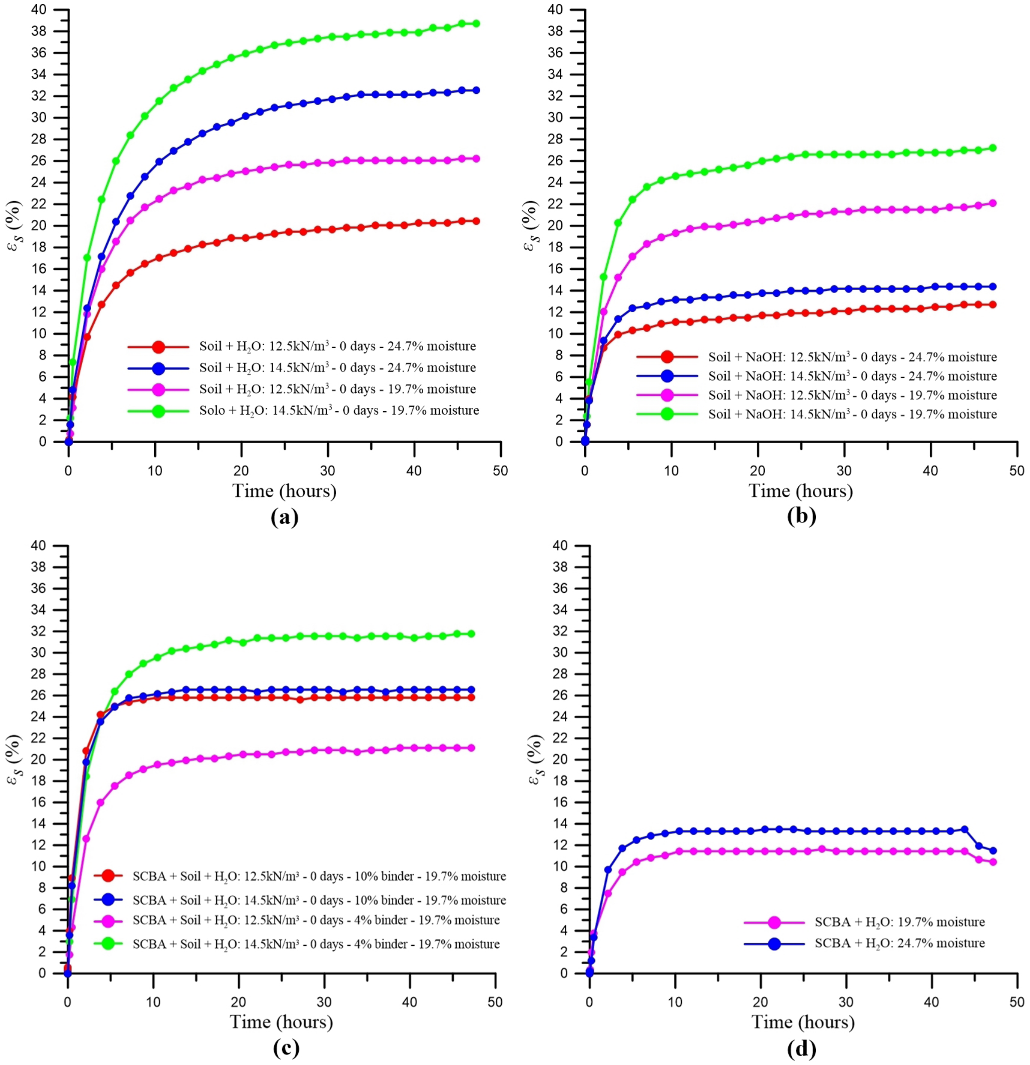

**Figure 4.** Free swelling results over time for samples containing (a) soil and water; (b) soil and NaOH; (c) SCBA, soil and water; and (d) only SCBA.

in higher expansion due to expansive soil particles higher concentration. For soil-alkali activated binder samples, there is not a clear correlation between higher density and higher expansion. However, alkali-activated samples with higher binder content showed a reduction in swell at higher density values. This is because the significant presence of NaOH in high-density low-binder content samples controlled swelling due to decrease in the bentonite diffuse double layer in the electrolyte nature (Reddy & Sivapullaiah, 2010).

In general, for both binders a higher curing time and binder content resulted in lower swelling, the exception being 4% binder content-7 days curing time alkali-activated samples. In the later, the precipitation of cementitious compounds (e.g. C-A-S-H and C-(N)-A-S-H gels) was not sufficient to counterbalance the bentonite (Figure 4a) and SCBA (Figure 4d) swell during the curing period (i.e. SCBA and bentonite swell disturbed the development of reaction products). However, in 10% binder content-7 days curing alkali-activated samples the precipitation of gels was higher. Thus, these products solidified, preventing bentonite and SCBA expansion during the curing period and after sample's submersion (e.g. treatments 15 and 16, Figure 2a, had almost no swell).

Swell reduced from 13.8% (12.5 kN/m$^3$ and 19.7% moisture) and 8.8% (12.5 kN/m$^3$ and 24.7% moisture) to 2.5% (82% reduction) and 0% (100% reduction), respectively, after 7 curing days and 10% binder addition for the alkali-activated binder. Syed et al. (2020) found similar results for an expansive clayey soil stabilized with fly ash activated by sodium hydroxide and sodium silicate: the swell percentage decreased 62% with 10% binder addition. For Portland cement, swell reduced from 13.8% (10.2 kN/m$^3$ and 22.5% moisture) and 12.5% (10.2 kN/m$^3$ and 27.5% moisture) to 1.8% (86% reduction) and 1% (92% reduction), respectively, after 7 curing days and 4% binder addition (Consoli et al., 2021).

In the Pareto chart, horizontal bars represent the effect magnitudes of each factor and bars exceeding the vertical line represent factors with significant influence over the response variable. The Pareto chart of alkali-activated samples (Figure 3a) shows that the binder content (*B*), second order interaction *BD* (binder content and curing time), and moisture content (*C*) posses, in this order, higher influence over swelling. For Portland cement (Figure 3b), the binder content (*B*), dry unit weight (*A*), and second order interaction *AB* possess, in this order, more influence over swelling. For both binders, the binder content (*B*) has more influence over swelling. This is mainly due to the precipitation of reaction products. Also, after the addition of those binders in soil, the *pH* of the environment increases leading to $Ca^{2+}$ release and cationic exchange between $Na^{+}$ and $Ca^{2+}$. The cation exchange followed by flocculation-agglomeration and pozzolanic reactions result in the formation of a coarse fabric which prevents swelling (Mitchell & Soga, 2005; Soltani et al., 2017).

For the main effects plot, the dotted line corresponds to the mean response of the tests, and line steepness is the effect intensity. Figure 3c,d shows that an increase on mean factors binder content, moisture content, and curing time reduced swelling. The higher line steepness of binder content denotes the higher influence of this factor. The middle points attest a non-linear behavior of the mean factors. In addition, for studied variables both binders presented a similar mean swell result (10%).

Figure 4 entails additional tests and corroborates previous conclusions; Figure 4b shows that samples containing NaOH expanded less than samples molded with only water (Figure 4a). This is explained by an increase in the *pH* in soil-NaOH samples (*pH* = 14) compared to soil-water samples (*pH* = 8.57). The *pH* increase might change the bentonite edge-face charge sign reducing soil fabric dispersion due to particle aggregation (Fan et al., 2013). In addition, a higher amount of cation in the environment, i.e. $Na^{+}$ from NaOH, causes shrinkage of the mineral's double-diffusion layer and flocculation of soil particle reducing swelling (Mitchell & Soga, 2005). Figure 4c shows that 4% SCBA-12.5 kN/m$^3$-19.7% moisture content (pink line) and 10% SCBA-14.5 kN/m$^3$-19.7% moisture content (blue line) soil samples, had a similar swell rate to soil-NaOH samples with same moisture content and density (pink and green lines of Figure 4b, respectively). However, other samples in Figure 4c swelled more than soil-NaOH samples with same moisture content and density. This is explained by Figure 4d: the SCBA swells over time.

## 4. Conclusion

This paper analyzed the swelling behavior of an expansive soil stabilized by an alkali-activated binder. Soil-Portland cement swell behavior was compared to the aforementioned binder. Free swelling tests and statistical analyses were performed. For both binders, the binder content had more influence over swelling. In addition, an increase on the main factors (binder content, moisture content, and curing time) reduced swelling. However, contrary to Portland cement specimens, soil-alkali activated binder samples no presented a clear correlation between higher density and higher expansion.

The significant presence of NaOH in high-density low-binder content alkali-activated samples controlled swelling; and soil-NaOH samples expanded less than samples molded with only distilled water. This is because *pH* increase might change the bentonite edge-face charge sign reducing soil fabric dispersion due to particle aggregation. For Portland cement, cementation of soil particles due to cement hydration reactions was the main responsible for swell reduction. For studied samples, swell reduced 100% and 91% with 10% alkali-activated binder and 4% Portland cement additions, respectively. Thus, aiming at swell reduction, Portland cement can be replaced by the alkaline binder, considering conditions similar to this study.

Although extensive research has been reported on the use of alkali-activation for soft soils (e.g. Abdullah et al., 2020; Cristelo et al., 2012; Liu et al., 2016; Phetchuay et al., 2016; Tonini de Araújo et al., 2023b; Zhang et al., 2013), few studies explored the use of these binders for swelling control. This study contributes to the literature by analyzing the use of alkali-activated wastes binder (SCBA and recycled eggshell) for a clayey soil stabilization. The utilized precursor expanded over time, and the activator controlled swelling. Thus, the influence of materials composing the alkali-activation binder on swelling should be carefully analyzed before any decision-making regarding soil stabilization.

## Acknowledgements

The present work was supported by CNPq - Conselho Nacional de Desenvolvimento Científico e Tecnológico – Brazil.

## Declaration of interest

The authors have no conflicts of interest to declare. All co-authors have observed and affirmed the contents of the paper and there is no financial interest to report.

## Authors' contributions

Mariana Tonini de Araújo: conceptualization, data curation, visualization, writing – original draft. Suéllen Tonatto Ferrazzo: conceptualization, data curation, methodology, validation, writing – original draft. Giovani Jordi Bruschi: conceptualization, data curation, methodology, validation, writing – original draft. Nilo Cesar Consoli: supervision, validation, writing – review & editing. The authors above kindly granted the permission of using parts of their publications in this template.

## Data availability

The datasets generated analyzed in the course of the current study are available from the corresponding author upon request.

## List of symbols and abbreviations

| | |
|---|---|
| *pH* | pH of soil-NaOH and soil-water samples |
| *A* | Dry unit weight |
| *AB* | Dry unit weight and binder content |
| *B* | Binder content |
| *BD* | Binder content and curing time |
| BT | Bentonite |
| *C* | Moisture content |
| CH | Inorganic clay of high plasticity |
| CL | Inorganic clay of low plasticity |
| CNPq | Conselho Nacional de Desenvolvimento Científico e Tecnológico |
| *D* | Curing time |
| $D_{50}$ | Main particle diameter |
| $H_0$ | Initial specimen height |
| HEL | Hydrated eggshell lime |
| K | Kaolin |
| *LL* | Liquid limit |
| OPC | Ordinary Portland cement |
| *PL* | Plastic limit |
| *PI* | Plasticity index |
| *S* | Degree of saturation |
| SCBA | Sugarcane bagasse ash |
| USCS | United soil classification system |
| $\Delta H$ | Specimen height change |
| $\varepsilon_s$ | Swell percentage |
| $\gamma_d$ | Density |

## References

Abdelkrim, M., & Mohamed, K. (2013). Cement stabilization of compacted expansive clay. *The Online Journal of Science and Technology*, 3(1), 33-38.

Abdullah, H.H., Shahin, M.A., Walske, M.L., & Karrech, A. (2020). Systematic approach to assessing the applicability of fly-ash-based geopolymer for clay stabilization. *Canadian Geotechnical Journal*, 57(9), 1356-1368.

ABNT NBR 15.895. (2010). *Materiais Pozolânicos – Determinação do Teor de Hidróxido de Cálcio Fixado – Método Chapelle Modificado*. ABNT - Associação Brasileira de Normas Técnicas, Rio de Janeiro, RJ (in Portuguese).

ABNT NBR 16605. (2017). *Cimento Portland e outros Materiais em Pó - Determinação da Massa Específica*. ABNT - Associação Brasileira de Normas Técnicas, Rio de Janeiro, RJ (in Portuguese).

Ahmadi Chenarboni, H., Lajevardi, S.H., MolaAbasi, H., & Zeighami, E. (2021). The effect of zeolite and cement stabilization on the mechanical behavior of expansive soils. *Construction and Building Materials*, 272, 121630.

ASTM D1557. (2012). *Standard Test Methods for Laboratory Compaction Characteristics of Soil Using Modified Effort (56,000 ft-lbf/ft3 (2,700 kN-m/m3))*. ASTM International, West Conshohocken, PA.

ASTM D4972. (2013). *Standard Test Method for pH of Soils*. ASTM International, West Conshohocken, PA.

ASTM D854. (2014a). *Standard Test Methods for Specific Gravity of Soil Solids by Water Pycnometer*. ASTM International, West Conshohocken, PA.

ASTM D4546. (2014b). *Standard Test Methods for One-dimensional Swell or Collapse of Soils*. ASTM International, West Conshohocken, PA.

ASTM D4318. (2017). *Standard Test Methods for Liquid Limit, Plastic Limit, and Plasticity Index of Soils*. ASTM International, West Conshohocken, PA.

ASTM D2487. (2020). *Standard Practice for Classification of Soils for Engineering Purposes (Unified Soil Classification System)*. ASTM International, West Conshohocken, PA.

ASTM D7928. (2021). *Standard Test Method for Particle-size Distribution (Gradation) of Fine-grained Soils Using the Sedimentation (Hydrometer) Analysis*. ASTM International, West Conshohocken, PA.

Boobalan, S.C., & Sivakami Devi, M. (2022). Investigational study on the influence of lime and coir fiber in the stabilization of expansive soil. *Materials Today: Proceedings*, 60, 311-314.

Bruschi, G.J., dos Santos, C.P., de Araújo, M.T., Ferrazzo, S.T., Marques, S., & Consoli, N.C. (2021a). Green stabilization of bauxite tailings: a mechanical study on alkali-activated materials. *Journal of Materials in Civil Engineering*, 33(11), 06021007.

Bruschi, G.J., dos Santos, C.P., Ferrazzo, S.T., De Araújo, M.T., & Consoli, N.C. (2021b). Parameters controlling loss of mass and stiffness degradation of "green" stabilised tailings. *Proceedings of the Institution of Civil Engineers - Geotechnical Engineering*, 176(3), 306-314.

Bruschi, G.J., dos Santos, C.P., Levandoski, W.M.K., Ferrazzo, S.T., Korf, E.P., Saldanha, R.B., & Consoli, N.C. (2022). Leaching assessment of cemented bauxite tailings through wetting and drying cycles of durability test. *Environmental Science and Pollution Research International*, 29, 59247-59262.

Buhler, R.L., & Cerato, A.B. (2007). Stabilization of Oklahoma expansive soils using lime and class C fly ash. In Puppala, A.J., Hudyma, N., & Likos, W.J. *Problematic soils and rocks and in situ characterization* (pp. 1-10). American Society of Civil Engineers.

Burris, L.E., Alapati, P., Moser, R.D., Ley, M.T., Berke, N., & Kurtis, K.E. (2015). *Alternative cementitious materials: Challenges and opportunities*. American Concrete Institute.

Carvalho Queiróz, L., Dias Miguel, G., Bruschi, G.J., & Deluan Sampaio de Lima, M. (2022). Macro–micro characterization of green stabilized alkali-activated sand. *Geotechnical and Geological Engineering*, 40, 3763-3778.

Consoli, N.C., Caicedo, A.M.L., Saldanha, R.B., Filho Scheuermann, C.H., & Acosta, C.J.M. (2020). Eggshell produced limes: innovative materials for soil stabilization. *Journal of Materials in Civil Engineering*, 32(11), 06020018.

Consoli, N.C., Tonini de Araújo, M., Ferrazzo, S.T., Rodrigues, V. de L., & da Rocha, C.G. (2021). Increasing density and cement content in stabilization of expansive soils: conflicting or complementary procedures for reducing swelling? *Canadian Geotechnical Journal*, 58(6), 866-878.

Cristelo, N., Glendinning, S., Fernandes, L., & Pinto, A.T. (2012). Effect of calcium content on soil stabilisation with alkaline activation. *Construction & Building Materials*, 29, 167-174.

Dang, L.C., Fatahi, B., & Khabbaz, H. (2016). Behaviour of expansive soils stabilized with hydrated lime and bagasse fibres. *Procedia Engineering*, 143, 658-665.

Duxson, P., Fernández-Jiménez, A., Provis, J.L., Lukey, G.C., Palomo, A., & Van Deventer, J.S.J. (2007). Geopolymer technology: the current state of the art. *Journal of Materials Science*, 42(9), 2917-2933.

Fan, R., Du, Y., Liu, S., & Chen, Z. (2013). Engineering behavior and sedimentation behavior of lead contaminated soil-bentonite vertical cutoff wall backfills. *Journal of Central South University*, 20, 2255-2262.

Fattah, M.Y., Salim, N.M., & Irshayyid, E.J. (2017). Influence of soil suction on swelling pressure of bentonite-sand mixtures. *European Journal of Environmental and Civil Engineering*, 26(7), 2554-2568.

Ferrazzo, S.T., Tonini de Araújo, M., Bruschi, G.J., Chaves, H.M., Korf, E.P., & Consoli, N.C. (2023a). Mechanical and environmental behavior of waste foundry sand stabilized with alkali-activated sugar cane bagasse ash-eggshell lime binder. *Construction & Building Materials*, 383, 131313.

Ferrazzo, S.T., Tonini de Araújo, M., Bruschi, G.J., Korf, E.P., Levandoski, W.M.K., dos Santos, C.P., & Consoli, N.C. (2023b). Metal encapsulation of waste foundry sand stabilized with alkali-activated binder: batch and column leaching tests. *Journal of Environmental Management*, 348, 119287.

Ferreira, S.R.M., Costa, L.M., Guimarães, L.J.N., & Pontes Filho, I.D.S. (2013). Volume change behavior due to water content variation in an expansive soil from the semiarid region of Pernambuco – Brazil. *Soils and Rocks*, 36(2), 183-193.

Gartner, E.M., & MacPhee, D.E. (2011). A physico-chemical basis for novel cementitious binders. *Cement and Concrete Research*, 41(7), 736-749.

Gaspar, T.A.V., Jacobsz, S.W., Heymann, G., Toll, D.G., Gens, A., & Osman, A.S. (2022). The mechanical properties of a high plasticity expansive clay. *Engineering Geology*, 303, 106647.

Goldoni, A.G., Pelissaro, D.T., Silveira, E., Prietto, P.D.M., & Dalla Rosa, F. (2023). Durability and mechanical long-term performance of reclaimed asphalt pavement stabilized by alkali-activation. *Soils and Rocks*, 46(1), e2023007422.

Indiramma, P., Sudharani, C., & Needhidasan, S. (2020). Utilization of fly ash and lime to stabilize the expansive soil and to sustain pollution free environment – An experimental study. *Materials Today: Proceedings*, 22, 694-700.

James, J. (2020). Sugarcane press mud modification of expansive soil stabilized at optimum lime content: Strength, mineralogy and microstructural investigation. *Journal of Rock Mechanics and Geotechnical Engineering*, 12(2), 395-402.

James, J., Roshna, R., & Santhiya, S. (2022). Cashew nut shell ash as a supplementary additive in lime stabilized expansive soil composites. *Materials Today: Proceedings*, 62, 644-649.

Khadka, S.D., Jayawickrama, P.W., Senadheera, S., & Segvic, B. (2020). Stabilization of highly expansive soils containing sulfate using metakaolin and fly ash based geopolymer modified with lime and gypsum. *Transportation Geotechnics*, 23, 100327.

Levandoski, W.M.K., Ferrazzo, S.T., Bruschi, G.J., Consoli, N.C., & Korf, E.P. (2023). Mechanical and microstructural properties of iron mining tailings stabilized with alkali-activated binder produced from agro-industrial wastes. *Scientific Reports*, 13, 15754.

Liu, Z., Cai, C.S., Liu, F., & Fan, F. (2016). Feasibility study of loess stabilization with fly ash–based geopolymer. *Journal of Materials in Civil Engineering*, 28(5), 04016003.

Mahedi, M., Cetin, B., & White, D.J. (2018). Performance evaluation of cement and slag stabilized expansive soils. *Transportation Research Record*, 2672(52), 164-173.

Miranda, T., Leitão, D., Oliveira, J., Corrêa-Silva, M., Araújo, N., Coelho, J., Fernández-Jiménez, A., & Cristelo, N. (2020). Application of alkali-activated industrial wastes for the stabilisation of a full-scale (sub)base layer. *Journal of Cleaner Production*, 242, 118427.

Mitchell, J.K., & Soga, K. (2005). *Fundamentals of soil behavior*. John Wiley & Sons.

Parhi, P.S., Garanayak, L., Mahamaya, M., & Das, S.K. (2018). Stabilization of an expansive soil using alkali activated fly ash based geopolymer. In L. Hoyos & J. McCartney (Eds.), *Advances in characterization and analysis of expansive soils and rocks* (pp. 36-50). Springer.

Pelissaro, D.T., Zago, A.A.C., Ferrazzo, S.T., Bruschi, G.J., & Dalla Rosa, F. (2023). Curing conditions effect on the stabilization of recycled asphalt pavement with alkali-activated metakaolin and rice husk ash-derived activator. *Road Materials and Pavement Design*, 1-7.

Pereira dos Santos, C., Bruschi, G.J., Mattos, J.R.G., & Consoli, N.C. (2022). Stabilization of gold mining tailings with alkali-activated carbide lime and sugarcane bagasse ash. *Transportation Geotechnics*, 32, 100704.

Phetchuay, C., Horpibulsuk, S., Arulrajah, A., Suksiripattanapong, C., & Udomchai, A. (2016). Strength development in soft marine clay stabilized by fly ash and calcium carbide residue based geopolymer. *Applied Clay Science*, 127-128, 134-142.

Phougat, N. (2015). Stabilization of expansive soil. *International Journal of Advance Engineering and Research Development*, 3(2), 24-34.

Queiróz, L.C., Batista, L.L.S., Souza, L.M.P., Lima, M.D., Danieli, S., Bruschi, G.J., & Bergmann, C.P. (2022). Alkali-activated system of carbide lime and rice husk for granular soil stabilization. *Proceedings of the Institution of Civil Engineers - Ground Improvement*, 176(5), 279-294.

Reddy, P.H.P., & Sivapullaiah, P.V. (2010). Effect of alkali solution on swell behavior of soils with different mineralogy. In *GeoFlorida 2010: Advances in Analysis, Modeling & Design* (pp. 2692-2701). Orlando.

Samuel, R., Puppala, A.J., & Radovic, M. (2020). Sustainability benefits assessment of metakaolin-based geopolymer treatment of high plasticity clay. *Sustainability*, 12(24), 10495.

Sahoo, S. & Prasad Singh, S. (2022). Strength and durability properties of expansive soil treated with geopolymer and conventional stabilizers. *Construction and Building Materials*, 328, 127078.

Secco, M.P., Mesavilla, D.T., Floss, M.F., Consoli, N.C., Miranda, T., & Cristelo, N. (2021). Live-scale testing of granular materials stabilized with alkali-activated waste glass and carbide lime. *Applied Sciences (Basel, Switzerland)*, 11(23), 11286.

Silvani, C., Lucena, L.C.D.F.L., Guimarães Tenorio, E.A., Filho, H.C.S., & Consoli, N.C. (2020). Key parameter for swelling control of compacted expansive fine-grained soil–lime blends. *Journal of Geotechnical and Geoenvironmental Engineering*, 146(9), 06020012.

Silvani, C., Guedes, J.P.C., da Silva, J.C., Tenório, E.A.G., & Nascimento, R.C.M. (2023). Brackish water in swelling soil stabilization with lime and sugarcane bagasse ash (SCBA). *Soils and Rocks*, 46(3), e2023010022.

Soltani, A., Taheri, A., Khatibi, M., & Estabragh, A.R. (2017). Swelling potential of a stabilized expansive soil: a comparative experimental study. *Geotechnical and Geological Engineering*, 35, 1717-1744.

Syed, M., GuhaRay, A., & Goel, D. (2022). Strength characterisation of fiber reinforced expansive subgrade soil stabilized with alkali activated binder. *Road Materials and Pavement Design*, 23(5), 1037-1060.

Syed, M., GuhaRay, A., & Kar, A. (2020). Stabilization of expansive clayey soil with alkali activated binders. *Geotechnical and Geological Engineering*, 38(6), 6657-6677.

Tonini de Araújo, M., Ferrazzo, S.T., Bruschi, G.J., & Consoli, N.C. (2021). Mechanical and environmental performance of eggshell lime for expansive soils improvement. *Transportation Geotechnics*, 31(2), 100681.

Tonini de Araújo, M., Ferrazzo, S.T., Bruschi, G.J., Silva, G.J.B., & Consoli, N.C. (2023a). Strength, mineralogy, microstructure and statistical analysis of alkali-activated sugarcane bagasse ash-eggshell lime pastes. *Journal of Materials in Civil Engineering*, 35, 04023107.

Tonini de Araújo, M., Ferrazzo, S.T., Chaves, H.M., da Rocha, C.G., & Consoli, N.C. (2023b). Mechanical behavior, mineralogy, and microstructure of alkali-activated wastes-based binder for a clayey soil stabilization. *Construction & Building Materials*, 362, 129757.

Yaghoubi, E., Yaghoubi, M., Guerrieri, M., & Sudarsanan, N. (2021). Improving expansive clay subgrades using recycled glass: resilient modulus characteristics and pavement performance. *Construction & Building Materials*, 302, 124384.

Yang, S., Wen, G., Yan, F., Li, H., Liu, Y., & Wu, W. (2020). Swelling characteristics and permeability evolution of anthracite coal containing expansive clay under water-saturated conditions. *Fuel*, 279, 118501.

Zhang, G., Yang, H., Ju, C., & Yang, Y. (2020). Novel selection of environment-friendly cementitious materials for winter construction: alkali-activated slag/Portland cement. *Journal of Cleaner Production*, 258, 120592.

Zhang, M., Guo, H., El-Korchi, T., Zhang, G., & Tao, M. (2013). Experimental feasibility study of geopolymer as the next-generation soil stabilizer. *Construction & Building Materials*, 47, 1468-1478.

Žurinskas, D., Vaičiukynienė, D., Stelmokaitis, G., & Doroševas, V. (2020). Clayey soil strength improvement by using alkali activated slag reinforcing. *Minerals (Basel)*, 10(12), 1076.